

Article

High-Pressure Synthesis, Structure, and Magnetic Properties of Ge-Substituted Filled Skutterudite Compounds; $Ln_xCo_4Sb_{12-y}Ge_y$, $Ln = La, Ce, Pr,$ and Nd

Hiroshi Fukuoka

Department of Applied Chemistry, Graduate School of Engineering, Hiroshima University, 1-4-1 Kagamiyama, Higashi-Hiroshima 739-8527, Japan; hfukuoka@hiroshima-u.ac.jp; Tel.: +81-82-424-7742

Academic Editor: Daniel Errandonea

Received: 18 October 2017; Accepted: 14 December 2017; Published: 15 December 2017

Abstract: A series of new Ge-substituted skutterudite compounds with the general composition of $Ln_xCo_4Sb_{12-y}Ge_y$, where $Ln = La, Ce, Pr,$ and Nd , is prepared by high-pressure and high-temperature reactions at 7 GPa and 800 °C. They have a cubic unit cell and the lattice constant for each compound is 8.9504 (3), 8.94481 (6), 8.9458 (3), and 8.9509 (4) Å for the La, Ce, Pr, and Nd derivatives, respectively. Their chemical compositions, determined by electron probe microanalysis, are $La_{0.57}Co_4Sb_{10.1}Ge_{2.38}$, $Ce_{0.99}Co_4Sb_{9.65}Ge_{2.51}$, $Pr_{0.97}Co_4Sb_{9.52}Ge_{2.61}$, and $Nd_{0.87}Co_4Sb_{9.94}Ge_{2.28}$. Their structural parameters are refined by Rietveld analysis. The guest atom size does not affect the unit cell volume. The Co–Sb/Ge distance mainly determines the unit cell size as well as the size of guest atom site. The valence state of lanthanide ions is 3+.

Keywords: skutterudite; intermetallic compound; high-pressure; thermoelectric materials

1. Introduction

The filled skutterudite compounds have attracted much attention after the finding of the anomalous superconductivity of $PrOs_4Sb_{12}$ [1]. It has a cage structure composed of corner-sharing MX_6 octahedra and large guest atoms A, which are situated in the cages, where A, M, and X are electropositive elements (mainly alkaline earth and rare earth elements), transition metals (group 8 and 9), and electronegative elements (mainly group 15), respectively. A lot of isotopic compounds were synthesized and examined to expand the skutterudite chemistry.

The high-pressure and high-temperature reactions are very effective to prepare new skutterudite compounds, including superconductors [2–5], and a great many filled skutterudite compounds have been reported for the widespread combination of the elements by the high-pressure techniques. Surprisingly, there are unique derivatives IM_4Sb_{12} , $M = Rh$ and Co , which have anionic guest atoms (iodine) in the cages [6–8]. Recently, bromine filled skutterudite has been reported [9].

The group 14 elements, however, are slightly difficult to introduce into the structure. Nolas et al. reported the first filled skutterudite compounds containing group 14 elements in the M site, $LnIr_4Sb_9Ge_3$, $Ln = La, Nd,$ and Sm . In these compounds, the electrons from the guest trivalent cations compensate for the electron deficiency of the host network caused by the substitution of a group 14 element for the group 15 element [10–12]. We also prepared a series of Ge-substituted filled skutterudite compounds $LnRh_4Sb_9Ge_3$, $Ln = La, Ce, Pr,$ and Nd , using high-pressure and high-temperature reactions [13]. They were stable at ambient pressure and the oxidation state of the guest atoms was 3+. Takizawa and Nolas also reported an interesting compound $Ge_{0.22}Co_4Sb_{11.4}Ge_{0.6}$, where germanium atoms were situated in the A site as well as in the X site [14].

In the present study, I used cobalt instead of Rh. Mori et al. also prepared a Ge-substituted skutterudite compound, which contains Yb in the Ln site, $Yb_yCo_4Sb_{11.5}Ge_{0.5}$ [15]. I performed high-pressure and high-temperature reactions in the Ln -Co-Sb-Ge system, $Ln = La, Ce, Pr,$ and Nd , to obtain a new series of Ge-substituted filled skutterudite compounds.

2. Results and Discussion

Dark gray products were obtained after the high-pressure reactions. They were stable in air under ambient pressure. The XRD patterns of obtained samples are shown in Figure 1. The diffractions for each compound were indexed with a cubic unit cell having the systematic absence of a space group $Im\bar{3}$. The peak pattern indicated that the obtained compounds have the skutterudite structure. Small amounts of Sb (containing small amount of Ge) and monoclinic $Co(Sb,Ge)_2$ were also detected as shown in the figure.

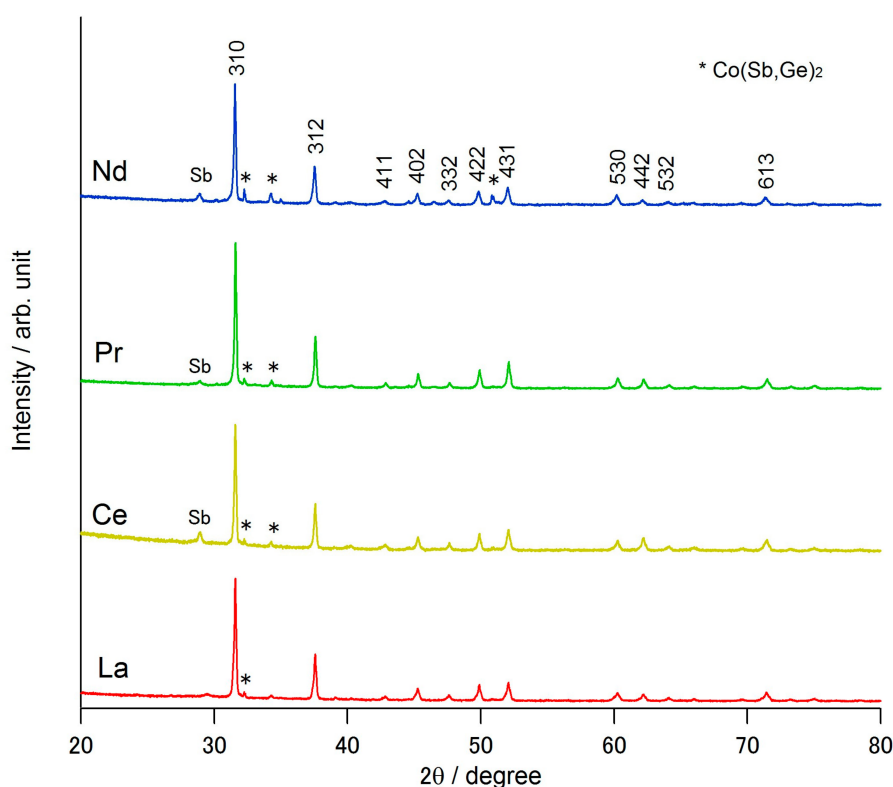


Figure 1. Powder XRD patterns of La, Ce, Pr, and Nd samples. The main phase is a Ge-substituted antimony skutterudite compound for each sample. Small diffraction peaks of Sb-Ge solid solutions and monoclinic $Co(Sb,Ge)_2$ are observed.

The presence of Ge in each compound was confirmed by chemical analysis. The chemical compositions for the samples determined by EPMA are summarized in Table 1. The relative number of atoms of each element is calculated according to an assumption that there is no defect in the Co site because the transition metal sites of the skutterudite structure are fully occupied in most skutterudite compounds. From these observations, the products of the high-pressure synthesis were identified as Ge-substituted filled skutterudite compounds.

I performed the Rietveld analysis for all compounds in order to confirm the site occupancy of the Ln sites and the Ge substitution for the Sb site. Rietveld structure analysis was performed using RIETAN-FP [16] on the powder XRD data collected with a D8 advance X-ray diffractometer (Bruker AXS, Karlsruhe, Germany) with $CuK\alpha$ radiation from 2θ range of 20° to 105° . The refined lattice

constant for each compound is shown in Table 1. The results of the pattern fitting in Rietveld analysis are shown in Figure 2.

Table 1. Lattice constant and chemical composition of Ge-substituted skutterudite compounds.

Composition	$\text{La}_{0.57}\text{Co}_4\text{Sb}_{10.1}\text{Ge}_{2.38}$	$\text{Ce}_{0.99}\text{Co}_4\text{Sb}_{9.65}\text{Ge}_{2.51}$	$\text{Pr}_{0.97}\text{Co}_4\text{Sb}_{9.52}\text{Ge}_{2.61}$	$\text{Nd}_{0.87}\text{Co}_4\text{Sb}_{9.94}\text{Ge}_{2.28}$
Lattice constant (Å)	8.9504 (3)	8.94481 (6)	8.9458 (3)	8.9509 (4)

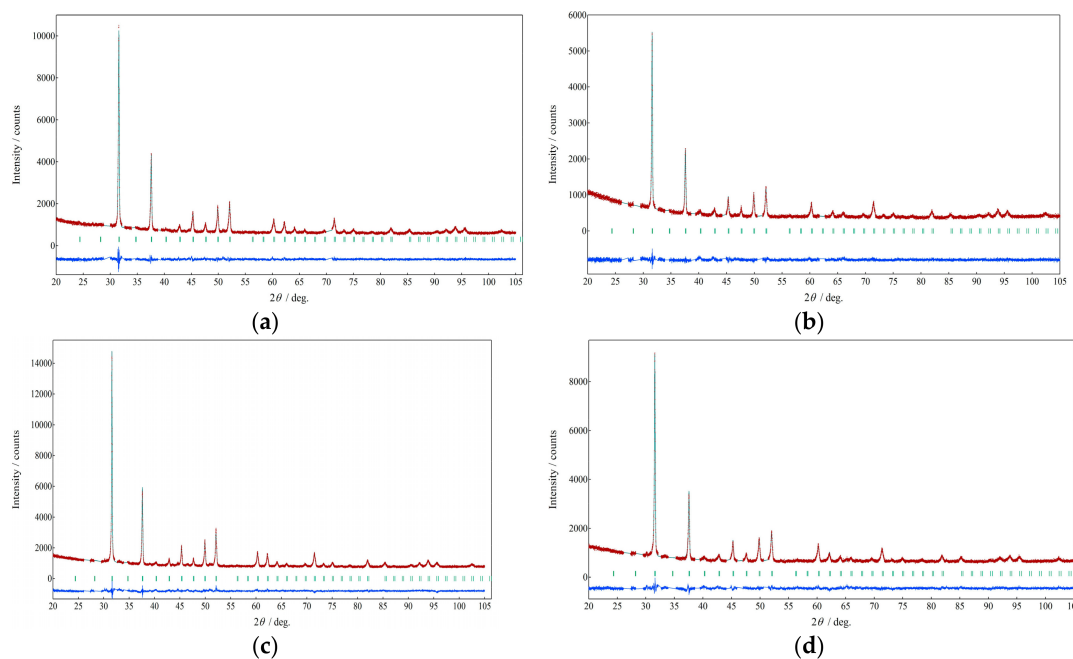


Figure 2. The XRD patterns and the results of pattern fitting; (a) $\text{La}_{0.57}\text{Co}_4\text{Sb}_{10.1}\text{Ge}_{2.38}$; (b) $\text{Ce}_{0.99}\text{Co}_4\text{Sb}_{9.65}\text{Ge}_{2.51}$; (c) $\text{Pr}_{0.97}\text{Co}_4\text{Sb}_{9.52}\text{Ge}_{2.61}$; (d) $\text{Nd}_{0.87}\text{Co}_4\text{Sb}_{9.94}\text{Ge}_{2.28}$. The observed data are shown as red points and the calculated fits and difference curves are shown as green and blue lines, respectively. Tick marks show the calculated diffraction positions.

All samples contain a very small amount of Sn-Ge solid solutions and monoclinic $\text{Co}(\text{Sb},\text{Ge})_2$ as shown in Figure 1. The diffraction peaks of those phases were excluded in Rietveld analysis so that they might not exert an adverse influence on the refinement.

The occupational parameters of *Ln* and Sb sites were refined as well as the atomic parameters and isotropic temperature factors for all sites. Split Pearson VII functions were used as profile functions. An overall isotropic temperature factor was refined only in the case of the La compound and a same isotropic temperature factor was applied to the Co and Sb/Ge sites only in the case of Ce compound due to the difficulty for convergence in the refinements.

The crystallographic data and some *R* factors are listed in Table 2. The atomic parameters and isotropic temperature factors for each compound are shown in Table 3. The refinement was well converged for each case. The *R* values are small and the *S* values are less than 1.3 for all compounds.

While the *Ln* sites of Ce, Pr, and Nd compounds were almost fully occupied, the La site occupancy turned out to be 0.7. I checked the possibility that some Ge atoms occupy the La site because some Ge atoms are situated in the guest site in a ternary skutterudite compound $\text{Ge}_{0.22}\text{Co}_4\text{Sb}_{11.4}\text{Ge}_{0.6}$ [14]. However, I could not get any meaningful results in all trials. I therefore concluded that the La site contained atom vacancies and did not contain any Ge atoms in the guest atom site. This site is fundamentally a site for cationic species in group 9–group 15 type skutterudite compounds. Therefore, if there is an electropositive element like La in the system, Ge appears not to be able to occupy the guest site.

The relatively larger isotropic temperature factors of the *Ln* sites may suggest an off-centered disorder of lanthanide ions. The analysis of it is, however, beyond the potential use of the present data.

The crystal structure of my compounds is illustrated in Figure 3. The refined occupational parameter of the *Ln* site for each compound is in good agreement with the composition determined by EPMA, when the standard deviations are taken into account. The M and X sites are occupied by cobalt and antimony atoms, respectively. Germanium atoms substituted randomly for some antimony atoms. The refined occupational parameters of the M site for the Ce and Pr compounds well reproduce the atomic ratios of Sb/Ge determined by EPMA, when the standard deviations are taken into account. Those parameters for La and Nd did not show good agreement with the Sb/Ge ratios determined by EPMA. This would be due to the fact that it is difficult to determine occupational parameters and temperature factors simultaneously. Especially in the case of the La compound, I applied an overall isotropic thermal parameter in the refinement, which might affect the poor estimation of the site occupancy of the La site. Even so, it can be clearly concluded that Ge atoms preferentially occupied the X site in the present systems.

Table 2. Crystallographic data and *R* indices of Rietveld analysis.

Formula	La _{0.57} Co ₄ Sb _{10.1} Ge _{2.38}	Ce _{0.99} Co ₄ Sb _{9.65} Ge _{2.51}	Pr _{0.97} Co ₄ Sb _{9.52} Ge _{2.61}	Nd _{0.87} Co ₄ Sb _{9.94} Ge _{2.28}
Space group	<i>I m-3</i> (204)	<i>I m-3</i> (204)	<i>I m-3</i> (204)	<i>I m-3</i> (204)
Lattice parameter (<i>a</i> /Å)	8.9504 (3)	8.94481 (6)	8.9458 (3)	8.9509 (4)
Unit cell volume <i>V</i> /Å ³	717.02 (4)	715.670 (9)	715.90 (4)	717.13 (6)
2θ range/degree	20–105	20–105	20–105	20–105
<i>R</i> _w /%	4.23	5.03	4.04	4.35
<i>R</i> _p /%	3.33	3.94	3.16	3.44
<i>R</i> _e /%	3.59	4.46	3.20	3.56
<i>R</i> _B /%	3.86	7.15	7.17	6.40
<i>R</i> _F /%	3.04	3.31	3.95	4.41
<i>S</i>	1.18	1.13	1.26	1.22

$R_{wp} = [\sum_i w_i \{y_i - I_i\}^2 / \sum_i w_i y_i^2]^{1/2}$, $R_p = \sum_i |y_i - I_i| / \sum_i y_i$, $R_e = [(N - P) / \sum_i w_i y_i^2]^{1/2}$, $R_B = \sum_k |I_k(o') - I_k(c)| / \sum_k I_k(o')$, $R_F = \sum_k \{ [I_k(o')]^{1/2} - [I_k(c)]^{1/2} \} / \sum_k [I_k(o')]^{1/2}$, $S = R_{wp} / R_e$; y_i : observed intensity, I_i : calculated intensity; w_i : weight; N : number of data; P : number of parameters; $I_k(o')$: estimated observed intensity of the *k*-th reflection; $I_k(c)$: calculated intensity of the *k*-th reflection.

Table 3. Structural parameters *ocp*, *n*, *x*, *y*, *z*, and *B*/Å² of the Ge-substituted cobalt antimony skutterudite compounds.

	<i>ocp</i>	<i>n</i> *	<i>x</i>	<i>y</i>	<i>z</i>	<i>B</i> /Å ²
La _{0.57} Co ₄ Sb _{10.1} Ge _{2.38}						
La	0.704 (8)	1.41	0	0	0	overall
Co	1	8	0.25	0.25	0.25	0.03 (5)
Sb	0.72 (2)	17.28	0	0.3396 (2)	0.1599 (2)	
Ge	0.28	6.72	0	0.3396	0.1599	
Ce _{0.99} Co ₄ Sb _{9.65} Ge _{2.51}						
Ce	0.90 (3)	1.78	0	0	0	2.8 (5)
Co	1	8	0.25	0.25	0.25	0.05 (4)
Sb	0.85 (2)	20.3	0	0.3384 (5)	0.1611 (3)	0.05
Ge	0.15	3.7	0	0.3384	0.1611	0.05
Pr _{0.97} Co ₄ Sb _{9.52} Ge _{2.61}						
Pr	0.94 (2)	1.88	0	0	0	3.0 (4)
Co	1	8	0.25	0.25	0.25	0.6 (3)
Sb	0.77 (5)	18.48	0	0.3408 (2)	0.1581 (2)	0.5 (1)
Ge	0.23	5.52	0	0.3408	0.1581	0.5
Nd _{0.87} Co ₄ Sb _{9.94} Ge _{2.28}						
Nd	0.87 (3)	1.74	0	0	0	5.6 (5)
Co	1	8	0.25	0.25	0.25	0.2 (3)
Sb	0.63 (4)	15.2	0	0.3376 (2)	0.1572 (2)	0.3 (2)
Ge	0.37	8.8	0	0.3376	0.1572	0.3

* *n*: number of equivalent atoms per unit cell.

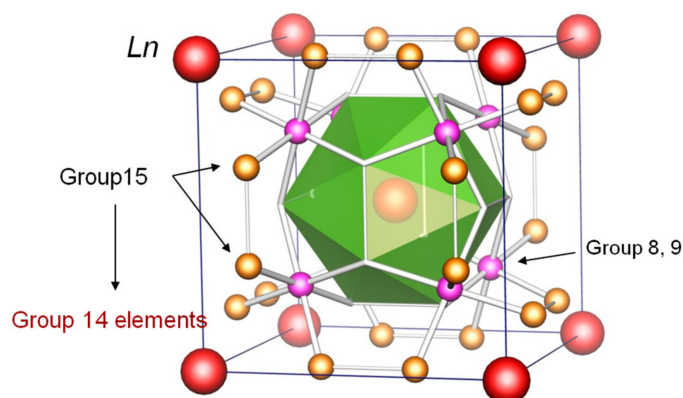


Figure 3. Crystal structure of the filled skutterudite compounds. In the present study, *Ln* sites are occupied by La, Ce, Pr, and Nd. The group 15 element is antimony, a part of which is substituted with germanium atoms. The transition metal sites are occupied by cobalt atoms.

The lattice constants of Ge-substituted compounds are smaller than that of CoSb_3 (9.039 Å [17]) because the radius of Ge is smaller than that of Sb. Figure 4 shows that the lattice parameter was not affected by the size of the guest ion, whether it was La, Ce, Pr, or Nd. They are almost constant. This means that the size of the unit cell is determined mainly by the covalent connection in the Co-(Sb,Ge) host network. Similar behavior was observed for the lattice constants of $\text{LnRh}_4\text{Sb}_9\text{Ge}_3$, $\text{Ln} = \text{La, Ce, Pr, and Nd}$ [10]. The lattice constants for those Rh compounds were in a very narrow range from 9.112 to 9.107 Å.

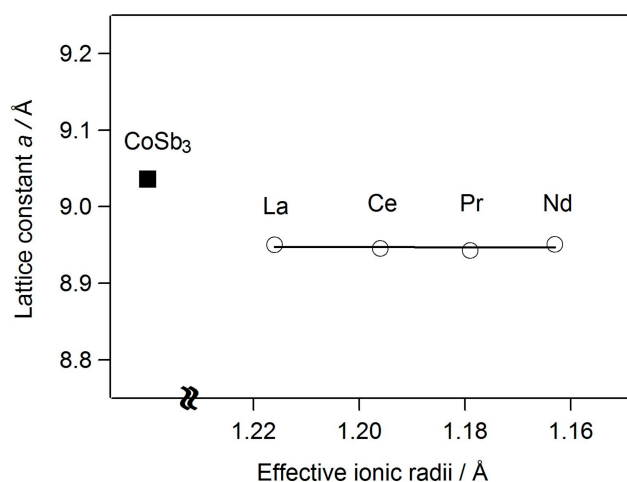


Figure 4. Lattice constant of the Ge-substituted cobalt skutterudite compounds.

The importance of the host network size is also proved by the fact that the lattice constants of the Ce and Pr compounds are slightly shorter than those of the La and Nd compounds. The former compounds contain a slightly larger amount of Ge in the X sites than the latter ones. The size of the host network is, thus, the principal parameter in these systems to determine the unit cell volume. This size effect of the host network also effectively explains the reason why it is difficult to prepare the analogs containing heavy rare earth elements, which have a smaller ionic radius than light ones. I tried to prepare a Lu analog by the same reaction condition but could not obtain it. Their small radius would not fit the host network size and such a system would become unstable. In contrast, the size of La^{3+} would be slightly too large for the cages. This indicates that difference of ionic size is why only the La site showed atomic vacancy.

The interatomic distances between host antimony/germanium atoms and guest Ln atoms are derived from the results of Rietveld analysis; they are 3.360, 3.353, 3.361, and 3.333 Å for the La, Ce, Pr, and Nd compounds, respectively. These values can be used as an indicator of the size of the A site. It is noteworthy that the interatomic distances of those compounds are very similar to that of $CoSb_3$ (3.352 Å [17]), even though the lattice constants of them remarkably decrease. Introduction of Ge atoms in the host network, therefore, contributes to the expansion of size of the A site, which can be correlated with the degree of f-electron localization in the lanthanide metal [18,19].

Magnetic susceptibility measurements revealed that the valence state of Ce and Nd was 3+. The temperature dependence of magnetic susceptibility of each compound is shown in Figure 5. The inset plots show Curie-Weiss behavior of the samples. Their susceptibilities obey a modified Curie-Weiss law, $\chi_{mol} = \chi_0 + C/(T - \theta)$, where χ_{mol} is a molar magnetic susceptibility, C is the Curie constant, θ is the Weiss temperature, and χ_0 is a paramagnetic term including a Van Vleck contribution. The data was approximated by the equation in the temperature range from 2 to 295 K for Ce and from 4 to 300 K for Nd. The obtained parameters in the fitting are summarized in Table 4. The effective moments calculated from their Curie constants are $2.12 \mu_B$ and $3.12 \mu_B$ for Ce and Nd, respectively. They are slightly smaller than the theoretical values of $2.54 \mu_B$ and $3.62 \mu_B$ for Ce^{3+} and Nd^{3+} . Although their valence states are basically 3+, we may have to consider mixed valence state or Kondo system especially for the Ce compound.

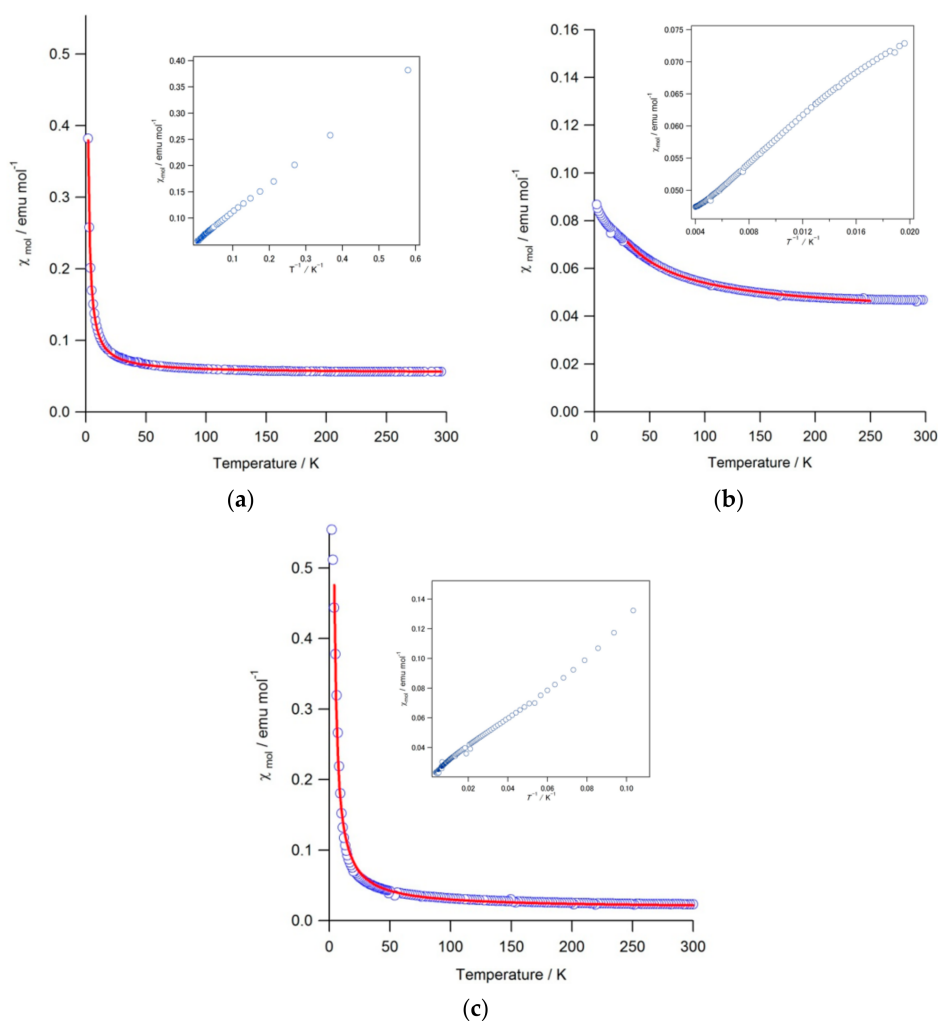


Figure 5. Temperature dependence of the magnetic susceptibility of (a) $Ce_{0.99}Co_4Sb_{9.65}Ge_{2.51}$; (b) $Pr_{0.97}Co_4Sb_{9.52}Ge_{2.61}$; and (c) $Nd_{0.87}Co_4Sb_{9.94}Ge_{2.28}$.

Table 4. Curie constant (C), Weiss temperature (θ), a paramagnetic term (χ_0) and the effective moment μ_{eff} (with theoretical values in parentheses) derived from regression calculations using a modified Curie-Weiss equation.

Compound	C (emu mol ⁻¹ K ⁻¹)	θ (K)	χ_0 (emu mol ⁻¹)	μ_{eff} (μ_B)	Temp. Range (K)
Ce _{0.99} Co ₄ Sb _{9.65} Ge _{2.51}	0.563 (3)	0.27 (1)	0.0544 (1)	2.12 (2.54)	2–295
Pr _{0.97} Co ₄ Sb _{9.52} Ge _{2.61}	1.78 (4)	−27 (1)	0.0401 (2)	3.77 (3.58)	30–250
Nd _{0.87} Co ₄ Sb _{9.94} Ge _{2.28}	1.22 (3)	1.33 (8)	0.0175 (7)	3.12 (3.62)	4–300

The data of the Pr compound did not obey the equation. I have, however, applied the equation to the data in a reduced temperature range from 30 to 250 K and obtained a well-fitting curve. The calculated effective moment of $3.77\mu_B$ is in good agreement with the theoretical value of $3.58\mu_B$ for Pr³⁺. The valence state of Pr would be 3+ in the temperature range; however, further investigation should be necessary to determine the magnetic behavior of the Pr compound as well as the Ce compound.

The partial substitution of Ge atoms for Sb atoms induces a structural disorder in the host network. Such a disorder would have an effect of decreasing the lattice thermal conductivity [10–12]. It is desirable to evaluate the thermal conducting and thermoelectric properties for these compounds.

3. Materials and Methods

In the sample preparation I used rare earth elements (99.9%, Rare Metallic Co., Ltd., Tokyo, Japan), cobalt powder (99.9%, Aldrich Chem. Co., St. Louis, MO, USA), antimony powder (99.999%, Katayama Chemical, Osaka, Japan), and germanium (99.999%, Rare Metallic Co., Ltd., Tokyo, Japan). I first prepared digermanides $LnGe_2$ for La, Ce, Pr, and Nd with an argon-filled arc furnace because the elemental lanthanides are highly unstable and are easily oxidized in air. The mixtures of $LnGe_2$, Co, Sb, and Ge with a molar ratio of 1:4:9:1 ($Ln:Co:Sb:Ge = 1:4:9:3$) were reacted using a Kawai-type (6–8 type) high-pressure system according to the following process [20]. Each mixture was placed in an h-BN container with 2 mm in inner diameter and 4 mm in depth. The container covered with Ta foil, which was used as a heater, was put in a thermal-insulating pyrophyllite tube with 6 mm in diameter and 1 mm thick. A Pt/Pt-Rh thermo couple was used to control the reaction temperature during heating. This sample unit was placed in an octahedral MgO pressure medium, and was put at the center of eight tungsten carbide anvils. This reaction cell was pressed by a multi-anvil press. The samples were reacted at 7 GPa and 800 °C for 1 h, and was rapidly cooled down to room temperature. After the sample temperature became room temperature, the pressure was slowly released.

All products were characterized by powder X-ray diffraction (XRD) method and electron probe micro analysis (EPMA) (JEOL 733II, Tokyo, Japan). Rietveld structure analysis was performed using RIETAN-FP [16] on the powder XRD data collected with a D8 advance X-ray diffractometer (Bruker AXS, Karlsruhe, Germany) with CuK α radiation from 2θ range of 20° to 105°. The magnetic susceptibility of the samples were measured with a SQUID magnetometer (Quantum Design MPMS5s, San Diego, CA, USA) applying a magnetic field of 5000 Oe.

4. Conclusions

High-pressure and high-temperature reactions provide a new series of Ge-substituted filled skutterudite compounds, $Ln_xCo_4Sb_{12-y}Ge_y$, where $Ln = La, Ce, Pr, \text{ and } Nd$. The guest site is fully occupied by lanthanide ions except for the La compound, whose occupancy x is 0.6. The germanium content, y , is different for each compound and is in the range from 2.3 to 2.6. The unit cell volume is not affected by the guest atom size. It is principally determined by the host network formed by the Co-Sb/Ge covalent bonds. The valence state of the guest lanthanide ions is basically 3+.

Acknowledgments: This work was supported by Grant-in-Aids for Scientific Research from the Ministry of Education, Science, and Culture of Japan, grant nos. 16037212, 16750174, 18750182, 18027010, 20550178, and 16K05724.

Conflicts of Interest: The author declares no conflict of interest.

References

1. Bauer, E.D.; Frederick, N.A.; Ho, P.-C.; Zapf, V.S.; Maple, M.B. Superconductivity and heavy fermion behavior in $\text{PrOs}_4\text{Sb}_{12}$. *Phys. Rev. B* **2002**, *65*, 1005061–1005064. [[CrossRef](#)]
2. Shirotani, I.; Shimaya, Y.; Kihou, K.; Sekine, C.; Yagi, T. Systematic high-pressure synthesis of new filled skutterudites with heavy lanthanide, $\text{LnFe}_4\text{P}_{12}$ (Ln = heavy lanthanide, including Y). *J. Solid State Chem.* **2003**, *174*, 32–34. [[CrossRef](#)]
3. Sekine, C.; Uchiyumi, T.; Shirotani, I.; Matsuhira, K.; Sakakibara, T.; Goto, T.; Yagi, T. Magnetic properties of the filled skutterudite-type structure compounds $\text{GdRu}_4\text{P}_{12}$ and $\text{TbRu}_4\text{P}_{12}$ synthesized under high pressure. *Phys. Rev. B* **2000**, *62*, 11581–11584. [[CrossRef](#)]
4. Kihou, K.; Shirotani, I.; Shimaya, Y.; Sekine, C.; Yagi, T. High-pressure synthesis, electrical and magnetic properties of new filled skutterudites $\text{LnOs}_4\text{P}_{12}$ (Ln = Eu, Gd, Tb, Dy, Ho, Y). *Mater. Res. Bull.* **2004**, *39*, 317–325. [[CrossRef](#)]
5. Shirotani, I.; Aresaki, N.; Shimaya, Y.; Nakata, R.; Kihou, K.; Sekine, C.; Yagi, T. Electrical and magnetic properties of new filled skutterudites $\text{LnFe}_4\text{P}_{12}$ (Ln = Ho, Er, Tm and Yb) and $\text{YRu}_4\text{P}_{12}$ with heavy lanthanide (including Y) prepared at high pressure. *J. Phys. Condens. Matter* **2005**, *17*, 4383–4391. [[CrossRef](#)]
6. Fukuoka, H.; Yamanaka, S. High-pressure synthesis, structure, and electrical property of iodine-filled skutterudite $\text{I}_{0.9}\text{Rh}_4\text{Sb}_{12}$ —First anion-filled skutterudite. *Chem. Mater.* **2010**, *22*, 47–51. [[CrossRef](#)]
7. Li, X.; Xu, B.; Zhang, L.; Duan, F.; Yan, X.; Yang, J.; Tian, Y. Synthesis of iodine filled CoSb_3 with extremely low thermal conductivity. *J. Alloys Compd.* **2014**, *615*, 177–180. [[CrossRef](#)]
8. Zhang, L.; Xu, B.; Li, X.; Duan, F.; Yan, X.; Tian, Y. Iodine-filled $\text{Fe}_x\text{Co}_{4-x}\text{Sb}_{12}$ polycrystals: Synthesis, structure, and thermoelectric properties. *Mater. Lett.* **2015**, *139*, 249–251. [[CrossRef](#)]
9. Ortiz, B.R.; Crawford, C.M.; McKinney, R.W.; Parillab, P.A.; Toberer, E.S. Thermoelectric properties of bromine filled CoSb_3 skutterudite. *J. Mater. Chem. A* **2016**, *4*, 8444–8450. [[CrossRef](#)]
10. Nolas, G.S.; Slack, G.A.; Caillat, T.; Meisner, G.P. Raman scattering study of antimony-based skutterudites. *J. Appl. Phys.* **1996**, *79*, 2622–2626. [[CrossRef](#)]
11. Nolas, G.S.; Slack, G.A.; Morelli, D.T.; Tritt, T.M.; Ehrlich, A.C. The effect of rare-earth filling on the lattice thermal conductivity of skutterudites. *J. Appl. Phys.* **1996**, *79*, 4002–4008. [[CrossRef](#)]
12. Tritt, T.M.; Nolas, G.S.; Slack, G.A.; Ehrlich, A.C.; Gillespie, D.J.; Cohn, J.L. Low-temperature transport properties of the filled and unfilled IrSb_3 skutterudite system. *J. Appl. Phys.* **1996**, *79*, 8412–8418. [[CrossRef](#)]
13. Fukuoka, H.; Yamanaka, S. High-pressure synthesis and structure of new filled skutterudite compounds with Ge-substituted host network; $\text{LnRh}_4\text{Sb}_9\text{Ge}_3$, Ln = La, Ce, Pr, and Nd. *J. Alloys Compd.* **2008**, *461*, 547–550. [[CrossRef](#)]
14. Nolas, G.S.; Yang, J.; Takizawa, H. Transport properties of germanium-filled CoSb_3 . *Appl. Phys. Lett.* **2004**, *84*, 5210–5213. [[CrossRef](#)]
15. Mori, H.; Anno, H.; Matsubara, K. Effect of Yb filling on thermoelectric properties of Ge-substituted CoSb_3 skutterudites. *Mater. Trans.* **2005**, *46*, 1476–1480. [[CrossRef](#)]
16. Izumi, F.; Momma, K. Three-dimensional visualization in powder diffraction. *Solid State Phenom.* **2007**, *130*, 15–20. [[CrossRef](#)]
17. Schmidt, T.; Kliche, G.; Lutz, H.D. Structure refinement of skutterudite-type cobalt triantimonide, CoSb_3 . *Acta Cryst. C* **1987**, *C43*, 1678–1679. [[CrossRef](#)]
18. Errandonea, D.; Boehler, R.; Schwager, B.; Mezouar, M. Structural studies of gadolinium at high pressure and temperature. *Phys. Rev. B* **2007**, *75*, 014103. [[CrossRef](#)]
19. Cunningham, N.C.; Qiu, W.; Hope, K.M.; Liermann, H.-P.; Vohra, Y.K. Symmetry lowering under high pressure: Structural evidence for f-shell delocalization in heavy rare earth metal terbium. *Phys. Rev. B* **2007**, *76*, 212101. [[CrossRef](#)]
20. Fukuoka, H. High-pressure and properties of new filled skutterudite compounds using a Kawai-type cell. *Rev. High Press. Sci. Technol.* **2006**, *16*, 329–335. [[CrossRef](#)]

